Generation of arbitrary terahertz wave forms in fanned-out periodically poled lithium niobate

J. R. Danielson, N. Amer, and Yun-Shik Lee[a)]

Department of Physics, Oregon State University, Corvallis, Oregon 97331-6507

The authors demonstrate a flexible terahertz pulse-shaping technique, manipulating spatially dispersed multifrequency components generated by optical rectification in a fanned-out periodically poled lithium niobate crystal. Spatial masks of low pass, high pass, and double slit in front of the crystal manipulate the spatial pattern of the optical excitation beam on the crystal, which is mapped onto the intensity profile of the terahertz spectrum. The spatial dispersion of the terahertz spectrum is removed by the line-to-point imaging of a spherical mirror. © *2006 American Institute of Physics.* [DOI: 10.1063/1.2392819]

Terahertz pulse shaping has many promising applications, for example, in high-speed optical signal processing,[1,2] ultrafast wireless digital interconnects,[3] biological and medical imaging,[4–6] and rotational and vibrational molecular dynamics.[7–9] Another intriguing application of shaped terahertz pulses is the coherent manipulation of quantum systems such as Rydberg atoms and Cooper pairs.[10,11] Carefully tailored terahertz pulses can also be utilized for coherent control of carrier dynamics in semiconductor nanostructures.

Several techniques to synthesize terahertz wave forms have been developed. These methods are based on either photoconductive switching or optical rectification. One approach to terahertz pulse shaping is to exploit orientation-inverted (OI) nonlinear optical media such as quasi-phase-matched (QPM) crystals. In this case, the terahertz wave form maps out the crystal domain structure. Tunable narrow-band terahertz generation was demonstrated by optical rectification in periodically poled lithium niobate (PPLN).[12–14] The basic concept of this method was applied to generate arbitrary terahertz wave forms in nonperiodic OI structures.[15,16] Recently, narrow-band terahertz pulses were produced in QPM GaAs structures.[17–19] The OI-crystal pulse shaping can cover broad temporal (0.1–200 ps) and spectral (0.1–5 THz) windows. Simultaneously, the spectral resolution is less than 0.01 THz and the temporal resolution is limited only by the optical pulse duration (<100 fs). The main limitation of this method is that the terahertz pulse shape is predetermined by the crystal domain structure; thus the pulse shaping is not adaptive. Another way of terahertz pulse shaping is to manipulate the temporal or spatial shapes of femtosecond optical pulses. Shaped ultrafast optical pulses in the time domain can irradiate nonlinear crystals or photoconductive switches to produce terahertz wave forms replicating the incident optical pulse envelope.[20,21] Spatially modulated optical pulses can manipulate the terahertz pulse shape in a lithium niobate crystal, and narrow-band terahertz pulses of Cherenkov radiation were generated by the transient polarization grating induced by two femtosecond pulses.[22] These techniques are adaptive because the optical pulse shapers allow active feedback. However, the quality of the pulse shaping is not as good as OI-crystal methods: the available time window is at best 10–20 ps and the corre-

sponding spectral resolution is about 0.1 THz. A hybrid technique combining the terahertz generation in PPLN with optical pulse shaping is not only adaptive but also has a broad time window.[23] The available bandwidth, however, is less than 0.1 THz.

In this letter, we demonstrate a terahertz pulse-shaping technique which is adaptive and includes all the favorable properties of the OI-crystal methods. With this technique we can have an ultimate control over the amplitude and phase of each frequency components in a terahertz pulse.

The schematic of this arbitrary pulse shaping technique is shown in Fig. 1(a). The terahertz emitter consists of a fanned-out (FO) PPLN crystal, a spatial mask, a cylindrical lens, and a spherical mirror. The domain width of the PPLN crystal varies continuously across the lateral direction; thus different regions emit terahertz radiation of different wave-
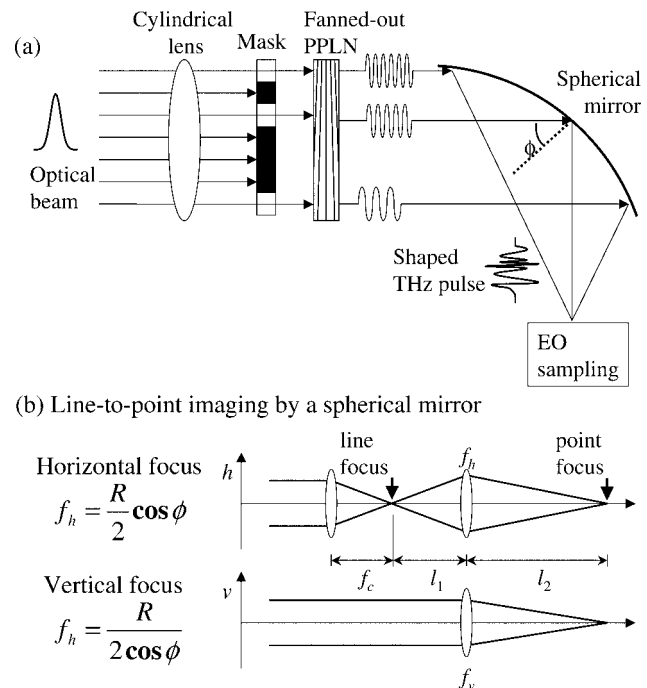

FIG. 1. (a) Experimental layout for arbitrary pulse shaping in a fanned-out PPLN crystal. ϕ is the incident angle of the terahertz beam on the spherical mirror. (b) Line-to-point imaging by a spherical mirror. f_h and f_v are horizontal and vertical focal length, respectively. R is the radius of curvature of the spherical mirror.

[a)]Electronic mail: leeys@physics.oregonstate.edu
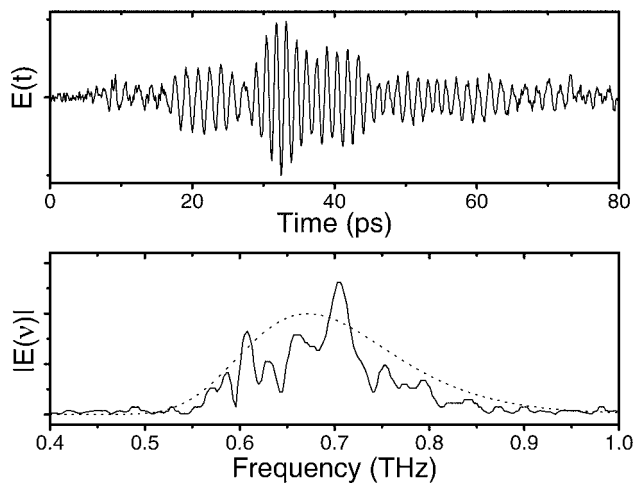
89, 211118-1

FIG. 2. Terahertz wave form and corresponding spectrum when no mask is inserted. The dotted line indicates the calculated spectrum for a 3-mm-wide gaussian beam.

lengths when illuminated. Optical pulses are line focused onto the FO-PPLN crystal to generate spatially separated multifrequency components of terahertz pulses. The spatial mask is placed in front of the FO-PPLN crystal in order to manipulate the spatial intensity pattern of the incident optical beam, thus controlling the amplitudes of the spatially dispersed terahertz frequency components. Spectral resolution of this method is determined by the FO-PPLN bandwidth and mask resolution: the estimated practical resolution is ~0.01 THz for a crystal with bandwidth of 1 THz. After the spherical mirror assembles the various frequencies into a single collimated beam, a shaped terahertz pulse can be obtained with the pulse shape determined by the Fourier transform of the pattern transferred by the mask. The beam collimation is accomplished by line-to-point imaging. We exploit the discrepancy between the vertical and horizontal focal lengths of the spherical mirror [Fig. 1(b)].

As a proof-of-principle experiment, we manipulated the terahertz wave forms with aluminum masks. The experiment was performed using 800 nm, 100 fs pulses from a 1 kHz Ti:sapphire regenerative amplifier (Legend, Coherent, Inc.). We used a 5-mm-long FO-PPLN sample (width=10 mm, height=0.5 mm) continuously tunable from 0.5 to 1.5 THz.[23] A cylindrical lens (f=10 cm) focused the pump beam (0.1 mJ pulse energy) into the FO-PPLN crystal with an elliptical beam profile of 3×0.3 mm^2. The optical pump beam generated a spatially dispersed spectrum of terahertz pulses: the bandwidth corresponding to the excited area of the FO-PPLN crystal should be ~0.2 THz as the central frequency is 0.67 THz. The line image of the terahertz beam in the crystal was focused to a point image by a spherical mirror (R=15 cm) with the incident angle ϕ=45°. Time-resolved terahertz wave forms were measured by electro-optic (EO) sampling in 1 mm ZnTe. Figure 2 shows the multicycle terahertz wave form without a mask and the corresponding spectrum. The spectrum is centered around 0.7 THz and ranges from 0.5 to 0.9 THz. The dotted line indicates the calculated spectrum for a Gaussian optical beam with 3 mm full width at half maximum. It is notable that the measured spectrum is not smooth. Domain structure imperfections may lead to the structure on the spectrum. The interference between different frequency components in the detection crystal is also a probable cause of it. All the fre-

quency components are collimated by the spherical mirror and spatially overlapped near the focal plane, but their propagation direction varies among different components. The structure on the spectrum may reflect the interference pattern in the wave form induced by the angular dispersion. It can also explain that the measured bandwidth (~0.2 THz) of the spectrum is slightly smaller than the calculation. EO sampling efficiency monotonically decreases with the angle between the optical and terahertz wave vector, where the optical probe beam is collinear with the terahertz wave at the central frequency (0.67 THz). Consequently, the measured spectrum is narrower than the calculated one. A terahertz grating at the focal plane can compensate for the angular dispersion; thus it may remove the spectral structure and recover the whole spectrum. Water absorption in the spectral region is a minor effect, but the two absorption lines at 0.5567 and 0.7518 THz are noticeable.

We placed metal masks before the PPLN crystal to block portions of the pump beam. This suppressed the terahertz generation by the covered regions, giving control over the emitted frequency spectrum. The first mask covered regions with a QPM period less than 160 μm, corresponding to a low-pass filter in the terahertz frequency domain. The second mask covered regions with a QPM period greater than 160 μm, correspond to a high-pass filter. The third mask was a double-slit filter, blocking illumination of portions of the crystal with a QPM period near 146 μm.

Figure 3 shows the measured and calculated terahertz wave forms determined by the spatial patterns of the masks and the corresponding spectra. The wave forms in Figs. 3(a-1), 3(b-1), and 3(c-1) are measured with 0.1 ps time step and 80 ps time window, which gives a spectral resolution of 0.0125 THz. The corresponding spectra [Figs. 3(a-3), 3(b-3), and 3(c-3)] were obtained by fast Fourier transform (FFT) of the wave forms. The spatial patterns of the masks are shown in the insets: blocked regions are in black. The gray lines indicate the unmasked spectrum. The numerically filtered spectra corresponding to the masks are shown in Figs. 3(a-4), 3(b-4), and 3(c-4). The wave forms in Figs. 3(a-2), 3(b-2), and 3(c-2) are the results of the inverse FFT of the calculated spectra. The low-pass filter blocks the high frequency parts (>0.65 THz) of the spectrum. The ensuing terahertz wave form in Fig. 3(a-1) is a long multicycle terahertz pulse. Consequently, the corresponding spectrum centered at 0.61 THz is narrow [Fig. 3(a-3)]: the bandwidth is about 0.02 THz. Figure 3(b-3) shows the spectrum of the high-pass filter, which blocks the frequency components lower than 0.65 THz. The terahertz wave form in Fig. 3(b-1) includes the main portion of the spectrum around 0.71 THz. The asymmetric waveform reflects the lopsided spectrum. The calculated wave forms [Fig. 3(a-2) and 3(b-2)] agree very well with the experimental results, which indicates that the phase distortion in the spectral filtering and spatial recombination is negligible. In Fig. 3(c), the double-slit mask suppresses the middle part of the spectrum, especially the main peak at 0.7 THz. This wave form is somewhat noisier as the most intense portion of the pump beam is blocked, decreasing the signal strength. Nonetheless, a 15 ps beating is clearly visible in the wave form, demonstrating interference between the lower and higher parts of the spectrum.

In conclusion, we have demonstrated a flexible scheme for terahertz pulse shaping. By selecting an OI crystal with a suitable range of QPM periods, we create a terahertz pulse

(a) Low-pass filter

(b) High-pass filter

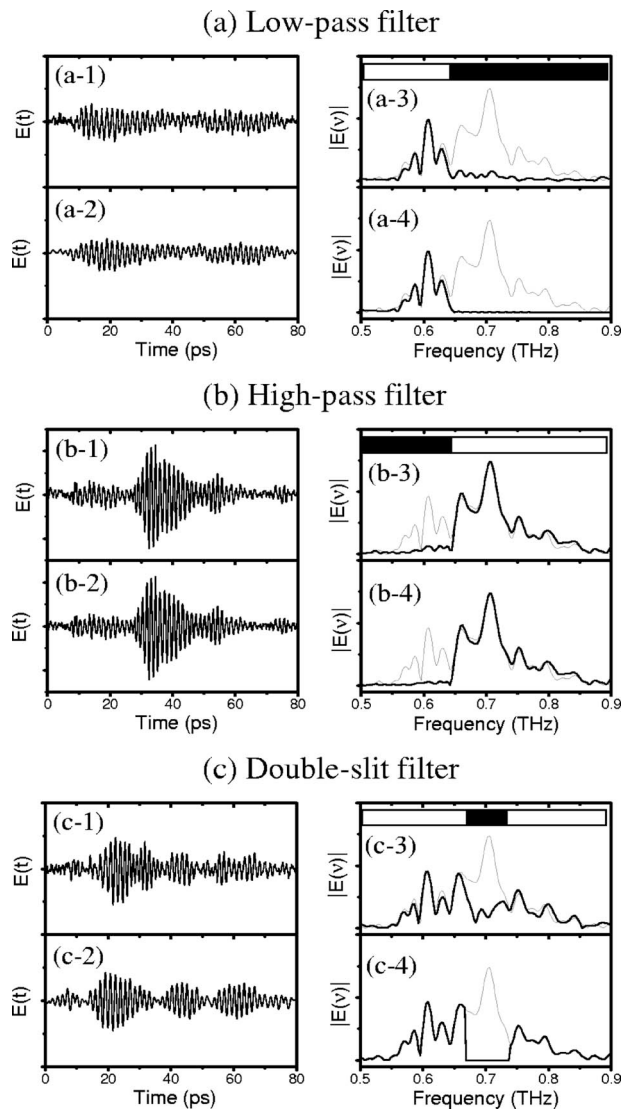

(c) Double-slit filter

FIG. 3. Measured and calculated terahertz wave forms and corresponding spectra with the metal masks: (a) high-pass filter, (b) low-pass filter, and (c) double-slit filter. [(a-1), (b-1), and (c-1)] measured wave forms; [(a-2), (b-2), and (c-2)] calculated wave forms; [(a-3), (b-3), and (c-3)] spectra of the measured wave forms; [(a-4), (b-4), and (c-4)] spectra of the calculated wave forms. The insets in [(a-3), (b-3), and (c-3)] show the spatial patterns of the masks scaled to the corresponding spectra. The gray lines in the spectra indicate the unmasked spectrum.

with a desired frequency range. Spatial filtering then allows us to suppress various portions of the spectrum, giving arbitrary control over the power spectrum. In particular, we have tested a low-pass, high-pass, and double-slit filter. All that

remains for full shaping of the waveform is to control the relative phases of the various terahertz components, which can be accomplished by varying their optical path length before recombination. Since the wavelengths of the terahertz radiation is in the hundreds of microns, this is well within the capabilities of micropositioning systems. Complicated phase patterning and amplitude modulation could be accomplished with a mirror array device such as a microelectromechanical system mirror. With a computer-controlled mirror array, one could create a feedback loop with the produced signal, allowing for adaptive pulse shaping.

[1] D. S. Citrin, Appl. Phys. Lett. **76**, 3176 (2000).
[2] M. Y. Su, S. G. Carter, M. S. Sherwin, A. Huntington, and L. A. Coldren, Appl. Phys. Lett. **81**, 1564 (2002).
[3] J. J. Simpson, A. Taflove, J. A. Mix, and H. Heck, Biotechnol. Bioprocess Eng. **14**, 343 (2004).
[4] P. Y. Han, G. C. Cho, and X.-C. Zhang, Opt. Lett. **25**, 242 (2000).
[5] D. D. Arnone, C. M. Ciesla, A. Corchia, S. Egusa, M. Pepper, J. M. Chamberlain, C. Bezant, and E. H. Linfield, Proc. SPIE **3828**, 209 (1999).
[6] J. L. Johnson, T. D. Dorney, and D. M. Mittleman, Appl. Phys. Lett. **78**, 835 (2001).
[7] C. Ronne, P. Strand, and S. R. Keiding, Phys. Rev. Lett. **82**, 2888 (1999).
[8] M. Brucherseifer, M. Nagel, P. H. Bolivar, and H. Kurz, Appl. Phys. Lett. **77**, 4049 (2000).
[9] E. Knoesel, M. Bonn, J. Shan, and T. F. Heinz, Phys. Rev. Lett. **86**, 340 (2001).
[10] Y. Nakamura, Yu. A. Pashkin, and J. S. Tsai, Nature (London) **398**, 786 (1999).
[11] J. Ahn, D. N. Hutchinson, C. Rangan, and P. H. Buchsbaum, Phys. Rev. Lett. **86**, 1179 (2001).
[12] Y.-S. Lee, T. Meade, V. Perlin, H. Winful, T. B. Norris, and A. Galvanauskas, Appl. Phys. Lett. **76**, 2505 (2000).
[13] Y.-S. Lee, T. Meade, M. DeCamp, T. B. Norris, and A. Galvanauskas, Appl. Phys. Lett. **77**, 1244 (2000).
[14] Y.-S. Lee, T. Meade, T. B. Norris, and A. Galvanauskas, Appl. Phys. Lett. **78**, 3583 (2001).
[15] Y.-S. Lee and T. B. Norris, J. Opt. Soc. Am. B **19**, 2791 (2002).
[16] Y.-S. Lee, N. Amer, and W. C. Hurlbut, Appl. Phys. Lett. **82**, 170 (2003).
[17] K. L. Vodopyanov, M. M. Fejer, X. Yu, J. S. Harris, Y.-S. Lee, W. C. Hurlbut, V. G. Kozlov, D. Bliss, and, C. Lynch, Appl. Phys. Lett. **89**, 14119 (2006).
[18] G. Imeshev, M. E. Fermann, K. L. Vodopyanov, M. M. Fejer, X. Yu, J. S. Harris, D. Bliss, and C. Lynch, Opt. Express **14**, 4439 (2006).
[19] Yum-Shik Lee, W. C. Hurlbut, K. L. Vodopyanov, M. M. Fejer, and V. G. Kozlov, Appl. Phys. Lett. **89**, 181104 (2006).
[20] J. Y. Sohn, Y. H. Ahn, D. J. Park, E. Oh, and D. S. Kim, Appl. Phys. Lett. **81**, 13 (2002).
[21] J. Ahn, A. V. Efimov, R. D. Averitt, and A. J. Taylor, Opt. Express **11**, 2486 (2003).
[22] A. G. Stepanov, J. Hebling, and J. Kuhl, Opt. Express **12**, 4650 (2004).
[23] W. C. Hurlbut, B. J. Norton, N. Amer, and Yun-Shik Lee, J. Opt. Soc. Am. B **23**, 90 (2006).